

See discussions, stats, and author profiles for this publication at: <https://www.researchgate.net/publication/38031973>

# Hybrid Heterojunction and Photoelectrochemistry Solar Cell Based on Silicon Nanowires and Double-Walled Carbon Nanotubes

ARTICLE *in* NANO LETTERS · OCTOBER 2009

Impact Factor: 13.59 · DOI: 10.1021/nl902581k · Source: PubMed

---

CITATIONS

58

READS

65

## 11 AUTHORS, INCLUDING:



Jinquan Wei

Tsinghua University

190 PUBLICATIONS 5,283 CITATIONS

[SEE PROFILE](#)



Kunlin Wang

Tsinghua University

206 PUBLICATIONS 4,938 CITATIONS

[SEE PROFILE](#)



Xinming Li

National Center for Nanoscience and Tech...

51 PUBLICATIONS 1,114 CITATIONS

[SEE PROFILE](#)

# Hybrid Heterojunction and Photoelectrochemistry Solar Cell Based on Silicon Nanowires and Double-Walled Carbon Nanotubes

Qinke Shu, Jinquan Wei, Kunlin Wang,\* Hongwei Zhu, Zhen Li, Yi Jia, Xuchun Gui, Ning Guo, Xinming Li, Chaoran Ma, and Dehai Wu

Key Laboratory for Advanced Materials Processing Technology and Department of Mechanical Engineering, Tsinghua University, Beijing 100084, People's Republic of China

Received August 7, 2009; Revised Manuscript Received September 23, 2009

## ABSTRACT

A hybrid solar cell model composed of a heterojunction cell and a photoelectrochemical (PEC) cell has been proposed and characterized. In the hybrid cell, a thin film of double-walled carbon nanotubes forms a heterojunction with the silicon nanowire (SiNW) array and also functions as the transparent counter electrode of the PEC cell. The cell performance can be readily tuned by controlling the SiNW density. Under AM 1.5G illumination, a power conversion efficiency of 1.29%, higher than those reported for SiNW array-based PEC cells, has been obtained.

Silicon is the most important semiconducting material in microelectronics, and silicon-based solar cells have played a dominant role in the photovoltaic market. Recently, silicon nanowires (SiNWs) especially SiNW arrays have attracted considerable research interest because of the potential applications in nanoelectronics and devices,<sup>1–3</sup> and the study of integrating SiNWs in solar cells has become a hot topic.<sup>4–11</sup> For example, vertically or slantingly aligned SiNW arrays have previously been assembled into homojunction solar cells,<sup>4,9</sup> representing an important step toward the utilization of the SiNW arrays in the field of solar cells, although the initial conversion efficiencies of these cells are comparatively low. Further effort used poly(3-octylthiophene) to fill the gaps between SiNWs, to facilitate the separation of photogenerated carriers on the whole surface of SiNWs,<sup>12</sup> however the conversion efficiency is still very low owing to the severe degradation of the poly(3-octylthiophene). Most recently, a photoelectrochemical (PEC) model has been introduced to the SiNW array-based solar cells,<sup>5–8</sup> and a high open-circuit voltage of 0.73 V and an improved conversion efficiency of 0.45% were obtained.<sup>8</sup> On one hand, the cell performance could be further improved by using low-cost conductive materials with high transparency as counter electrodes. On the other hand, the internal resistance could be reduced by reducing the gap between the counter electrode and the SiNW array. For this purpose, carbon nanotubes

(CNTs) could be an ideal candidate. CNTs have been integrated in flexible transparent conductive films<sup>13–15</sup> and embedded in organic materials<sup>16–18</sup> or other semiconductors,<sup>19</sup> to facilitate the separation and transport of photogenerated carriers. In particular, CNTs and silicon can form heterojunctions,<sup>20</sup> and solar cells based on such CNT/silicon heterojunctions have produced a high efficiency of 7%.<sup>21,22</sup> Thus, it is expected that the integration of the SiNW array and CNTs could lead to high-performance solar cells by a concurrent action of the SiNW array-based PEC cell and the CNTs/SiNWs heterojunction cell.

In this Letter, we demonstrate such a hybrid solar cell consisting of two types of photovoltaic structures, a heterojunction cell and a PEC cell connected in parallel, as illustrated in Figure 1. Figure 1a shows the three main components, the SiNW array, the double-walled carbon nanotube (DWNT) thin film, and the redox electrolyte (HBr and Br<sub>2</sub>). The DWNT film was conformally transferred onto the top surface of the SiNW array, to form heterojunctions with the SiNWs. Photoexcited charge carriers generated in the SiNW array are separated by the built-in field, where electrons are directed to the n-type Si region (red arrows) and holes move toward the DWNT film (yellow arrows). The DWNT film also acts as a percolated network that is favorable for charge collection and transport. Meanwhile, the SiNW arrays and the redox electrolyte also create a PEC cell with the DWNT film as the counter electrode. In a typical photochemical process, the holes driven to the SiNW surface

\* To whom correspondence should be addressed: wangkl@mail.tsinghua.edu.cn; tel, +86-10-62792845; fax, +86-10-62770190.

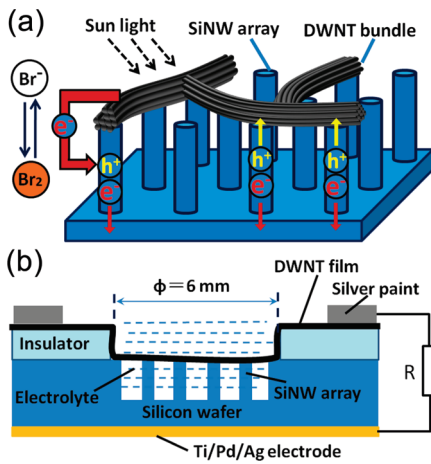


**Figure 1.** (a) Hybrid heterojunction/PEC solar cell composed of SiNW arrays, the DWNT film, and the redox electrolyte. (b) Side view of the hybrid structure.

are scavenged by oxidizing  $2\text{Br}^-$  to  $\text{Br}_2$ . The  $\text{Br}_2$  diffuses to the DWNT film where it is reduced back to  $2\text{Br}^-$ .

The SiNW arrays were first prepared using n-type (100) silicon wafers (with a sheet resistance of  $2\text{--}4 \Omega \text{ cm}$ ) by a Ag-assisted etching method<sup>4,23</sup> and then treated in a HF and  $\text{HNO}_3$  aqueous solution for different periods of time (see Supporting Information), to form sparse SiNWs. The as-fabricated SiNWs are single crystalline and mainly 20–150 nm in diameter. The SiNW arrays were cut into pieces of  $1.2 \times 1.2 \text{ cm}^2$ . Insulating tape ( $1.2 \times 1.2 \text{ cm}^2$ ) with a round window (6 mm diameter) was adhered on the top surface of the SiNW array (see Figure 1b). Smooth, homogeneous, macroscopic DWNT thin films were prepared as reported in our previous work<sup>24</sup> and conformally transferred to the top of the SiNW array. SiNW arrays with three different SiNW densities (0.150, 0.100, and 0.050, defined as the gross cross section area of the SiNWs divided by the area of the Si substrate) were tested in this study.

Redox electrolyte containing 40% hydrobromic acid and 3% bromine was dropped on the DWNT film from the round window, forming a film with an average thickness of 0.7 mm. The upper electrode was connected to the DWNT film by silver paint (separated from the underlying SiNWs by the insulating tape). A Ti/Pd/Ag layer was sputtered at the back side of the silicon substrate as the back electrode. Forward bias is defined as positive voltage applied to the DWNT film. The devices were irradiated under a solar simulator (Thermo Oriel 91192-1000) at AM 1.5G ( $100 \text{ mW/cm}^2$ ), and the current–voltage data were recorded using a Keithley 4200 sourcemeter. The spectral photoresponse of the hybrid solar cell was also measured (CEP-25/CH). The SiNW arrays and DWNT films were characterized by scanning electron microscope (SEM, LEO 1530). The transmission spectra of the DWNT film and the redox electrolyte and the reflection spectrum of the SiNW array were characterized by a UV-vis spectrometer (Lambda 950).

SEM characterization reveals that the etching profile is uniform with a depth of ca.  $5 \mu\text{m}$  (Figure 2a). Figure 2b shows a network structure of the as-coated DWNT film that

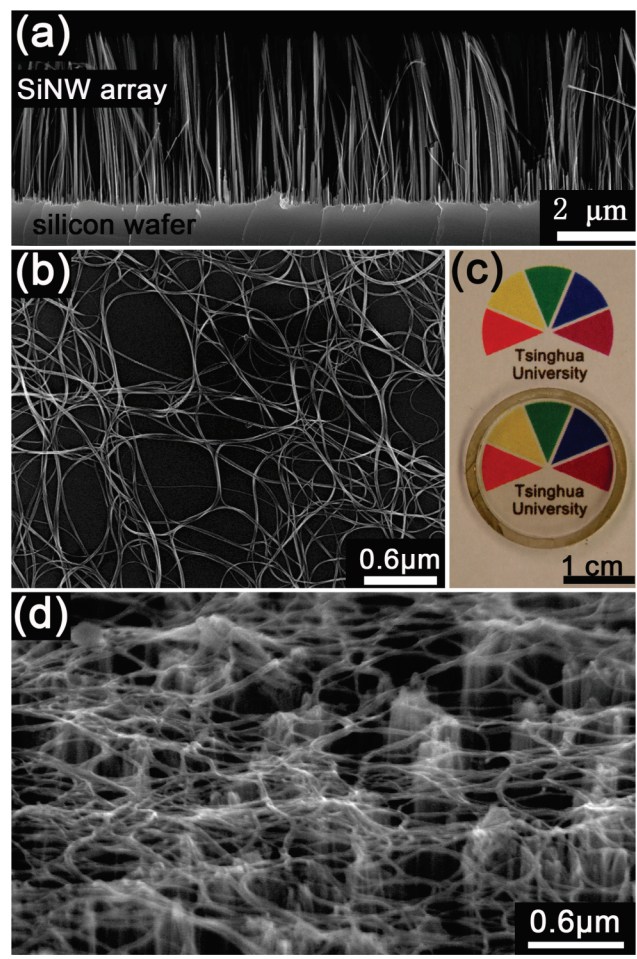


**Figure 2.** Morphological characterizations of the SiNW array and the DWNT film. (a) SEM image of the cross section of the SiNW array. (b) SEM image of the DWNT film. (c) A single-layer DWNT film collected on a quartz O-ring, through which the background colors can be seen clearly. (d) SEM image of the top view of the DWNT film/SiNW array interface.

is free of impurities. The film is highly transparent, and the color painting underneath is clearly visible (Figure 2c). Figure 2d is the top view of the DWNT film of about 50 nm thick on top of the SiNW array.

Without redox electrolyte, the SiNW array and DWNT film form a heterojunction (sample A1). In Figure 3a, curve A1 shows the current density–voltage ( $J$ – $V$ ) characteristics of the SiNW array/DWNT heterojunction under AM 1.5G illumination, with a low conversion efficiency ( $\eta$ ) of 0.092% and a fill factor (FF) of 0.12. Upon addition of the redox electrolyte, the cell (sample A2) performance is significantly improved, exhibiting relatively high open-circuit voltage ( $V_{oc}$ ), short-circuit current density ( $J_{sc}$ ), and FF of 0.50 V,  $10.5 \text{ mA/cm}^2$ , and 0.25, respectively. The corresponding efficiency  $\eta$  increased to 1.29%. It is possible that the redox electrolyte and the SiNW array created a PEC cell while the DWNT film acted as the counter electrode. The SiNWs have very large specific surface areas, which made the effective contact surfaces between the redox electrolyte and SiNWs much bigger. Hence, the carrier separation could take place in the radial direction rather than the axial direction, so that the carrier collection distance is much smaller, comparable

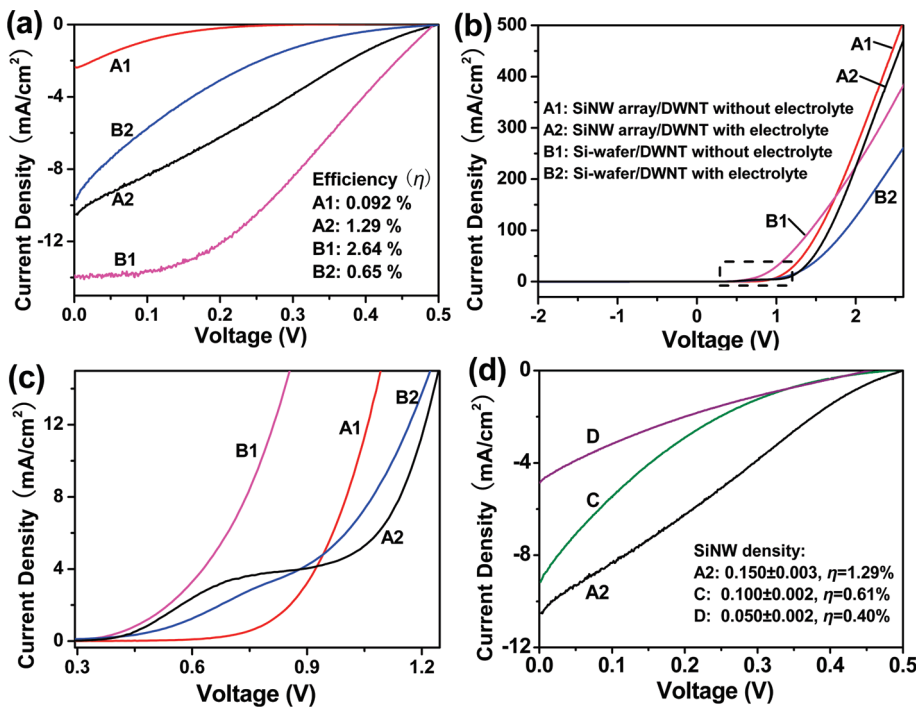


**Figure 3.** (a) Light (AM 1.5G) and (b) dark  $J-V$  curves of the Si/DWNT solar cells. (c) An enlarged view of the rectangle region marked in (b). (d) Light  $J-V$  curves of the hybrid solar cells with different SiNW densities.

to the minority carrier diffusion length. Therefore, the enhancement of efficiency may be attributed to the presence of the redox electrolyte filling the SiNW gaps. The conversion efficiency of the hybrid cell is higher than those of previously reported SiNW array-based PEC solar cells,<sup>6,8</sup> in which thin platinum layers were used as counter electrodes which did not contact the SiNW arrays directly. Two reasons may account for the enhanced overall performance: (i) the strong adhesion between the DWNT film and the SiNW array which greatly reduces the series resistance; (ii) the highly transparent DWNT film which enables good light transmission onto the SiNW arrays.

To understand the actual role of the SiNW array in the solar cell, a silicon wafer/DWNTs heterojunction solar cell (sample B1) was also compared for comparison. As shown in curve B1 of Figure 3a, the cell displays a relatively higher  $\eta$  of 2.64%. However, the efficiency dropped sharply to 0.65% (curve B2) after the redox electrolyte was introduced. This result indicates that the SiNW arrays have a better PEC performance than silicon wafer in hybrid cells when redox electrolyte was involved.

Figure 3b shows the dark  $J-V$  characteristics of samples A1, A2, B1, and B2. All four samples exhibited convincing p-n junction behaviors in the dark with high rectification ratios of over 1000 at 2 V. The on-voltage for sample A1 is higher than that of B1, Figure 3c, possibly because the DWNT film contact with the SiNW arrays was not as good as that with the silicon wafer. Curve A2 shows a reverse-S shape, representing two on-voltages. The lower on-voltage ( $\sim 0.4$  V), which is lower than the on-voltage of A1, arises from the PEC reaction. The higher on-voltage ( $\sim 1.0$  V) is associated with the SiNW array/DWNT film heterojunctions. This result demonstrates that the heterojunction cell works

well in the presence of redox electrolyte. The combined role of these two cells leads to increased conversion efficiency. On the contrary, the addition of redox electrolyte has a negative effect on the cell performance of sample B2, with comparison to B1. For example, at 0.6 V, the current density of B1 reached 3.5  $\text{mA}/\text{cm}^2$ , but only reached 1.5  $\text{mA}/\text{cm}^2$  for B2. This phenomenon is associated with the light  $J-V$  curves of samples B1 and B2, as revealed in Figure 3a. The silicon wafer and DWNT film can form a good heterojunction for power conversion, but the presence of redox electrolyte would allow for the charge carriers to recombine, reducing the conversion efficiency. The presence of redox electrolyte in a PEC cell can improve the conversion efficiency, but such enhancements cannot compensate for the adverse effect of reducing efficiency, due to the small surface area of the silicon wafer compared with the SiNW arrays. Thus the performance of sample B2 with redox electrolyte is far poorer than that of B1. These  $J-V$  characteristics of samples A1 and A2 also clearly demonstrate that the presence of the redox electrolyte indeed resulted in a hybrid cell composed of a heterojunction cell and a PEC cell which are connected in parallel.

Hybrid solar cells with different SiNW densities (0.150, 0.100, and 0.050) were further characterized. The light  $J-V$  curves of these cells under illumination of AM 1.5G are shown in Figure 3d, and the corresponding photovoltaic data are summarized in Table 1. At low density, the  $V_{oc}$  only decreases slightly from 0.50 to 0.45 V, while the  $J_{sc}$  decreases significantly from 10.5 to 4.86  $\text{mA}/\text{cm}^2$ , and the  $\eta$  also drops from 1.29% to 0.40%. Three reasons may account for the phenomenon. First, the SiNW array with low reflection could absorb more solar light and generate more charge carriers;<sup>8,25</sup> however, the reflection would increase as the SiNWs become

**Table 1.** Photovoltaic Parameters for Si/DWNT Solar Cells under AM 1.5G Simulated Illumination

sample	SiNW density	specific surface area ( $\text{m}^2/\text{m}^3$ )	$V_{\text{oc}}$ (V)	$J_{\text{sc}}$ ( $\text{mA}/\text{cm}^2$ )	fill factor	$\eta$ (%)
A2	$0.150 \pm 0.003$	$\sim 6.5 \times 10^6$	0.50	10.5	0.25	1.29
C	$0.100 \pm 0.002$	$\sim 5.6 \times 10^6$	0.48	9.16	0.14	0.61
D	$0.050 \pm 0.002$	$\sim 4.1 \times 10^6$	0.45	4.86	0.18	0.40

sparse. Second, surface areas of the SiNWs decreased as SiNWs became sparse, which was not favorable for the charge separation and collection. Finally, sparse SiNWs led to comparatively small contact area between DWNT film and SiNW array, which may also affect the solar cell performances.

The results of the quantum efficiency ( $Q$ ), the photocurrent spectrum normalized to the incident photon flux, are shown in Figure 4a. The  $Q$  maxima of A1 and A2 occur at 1.35 eV ( $\sim 920$  nm). The inset of Figure 4a shows the relationship between the energy and the energy derivative of  $Q$ , with peaks at 1.13 and 1.19 eV for A1 and A2, respectively. The peaks are close to the energy band gap of silicon (1.12 eV), signifying the dominant contributions of SiNW arrays to the absorption of most incident photons and to the generation of charge carriers. The DWNT film is highly transparent (Figure 4b), with a transmission of  $>60\%$  in the visible range. Though the light absorbed by the DWNT film can generate charge carriers,<sup>26</sup> its contribution to the photocurrent is limited. Sample A1 without redox electrolyte shows a very low photocurrent which mainly arises from the SiNW array (as shown in Figure 4a). Both the DWNT film and redox electrolyte are highly transparent in the range of 600–1150 nm, and the reflection of the SiNW array is very low (<5%) compared with that of the silicon wafer, which allows most of the light in the range to be absorbed by the SiNW arrays.

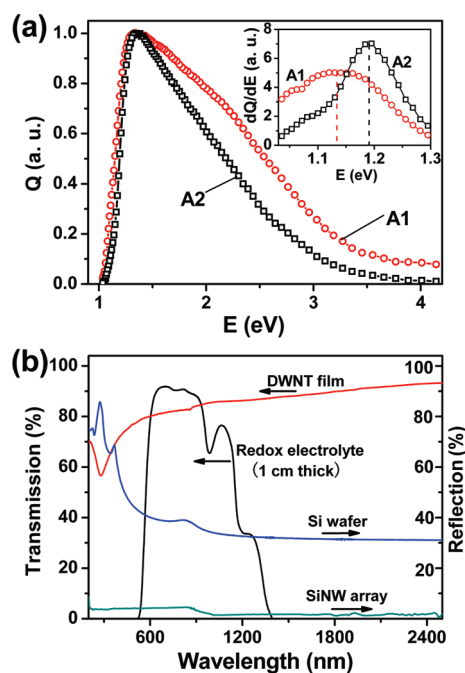


**Figure 4.** (a) Plots of the quantum efficiency ( $Q$ ) vs photon energy ( $E$ ) measured from samples A1/A2. The inset shows the plots of the energy derivative of  $Q$  vs photon energy  $E$ . (b) The optical data of the solar cell components.

However, in the ranges of <600 nm and >1200 nm, the redox electrolyte is nearly opaque, which partly suppresses the absorption of light by the SiNW arrays. Therefore the full width at half-maximum of curve A1 in Figure 4a is larger than that of curve A2.

For further improvement, three possible ways could be explored to enhance the efficiency of the hybrid solar cell. First, the as-prepared DWNT film consists of both semiconducting and metallic nanotubes.<sup>27</sup> A higher efficiency is expected with higher percentage of semiconducting DWNTs in the film. Second, the composition of the redox electrolyte solution would affect the series resistance and the separation process of the photogenerated carriers. Further optimization of the redox electrolyte is needed. Finally, the height of the SiNW arrays defines the surface areas of the SiNWs which may have strong influence on the conversion efficiency. Furthermore, the cost of the hybrid solar cell is competitive, and low-cost fabrication of CNT films in large quantity could be helpful for application in this field.<sup>28</sup> The SiNW arrays were made from a silicon wafer which is expensive; however, the process can be replaced directly by a vapor–liquid–solid (VLS) technique<sup>29,30</sup> or etching silicon thin film on glass.<sup>10</sup> Hence, it is believed that the hybrid solar cell is a potentially exciting model for future research and application.

In summary, this Letter has demonstrated that at the presence of the redox electrolyte, SiNW arrays, and DWNT film formed a hybrid solar cell of heterojunction and photoelectrochemistry. The DWNT film formed heterojunctions with the SiNW arrays and also acted as the transparent counter electrode in the PEC cell, at the same time. The low reflective SiNW arrays generated most of the charge carriers, and the presence of the redox electrolyte in the gap between SiNWs facilitated the collection of carrier from the surface of SiNWs. At SiNW density of 0.150, the hybrid solar cell shows a relatively high conversion efficiency of 1.29%.

**Acknowledgment.** This work was financially supported by NSFC (Grant No. 50672047), National High Technology Research and Development Program (2009AA05Z423), and Key Project of Ministry of Education (No. 108006), China. We acknowledge the support of Ying Xu and Shuang Song for electrode fabrication and Professor Kuiqing Peng for SiNWs preparation. We also thank Professor Daming Zhuang, Professor Gong Zhang, Professor Liduo Wang, and Chunlei Li for electrical testing and useful discussions.

**Supporting Information Available:** (i) Details of the fabrication of the hybrid solar cell and (ii) parameters of all the solar cells mentioned in the paper. This material is available free of charge via the Internet at <http://pubs.acs.org>.

## References

- (1) Cui, Y.; Lieber, C. M. *Science* **2001**, *291*, 851–853.
- (2) Ma, D.; Lee, C. S.; Au, F.; Tong, S. Y.; Lee, S. T. *Science* **2003**, *299*, 1874–1877.
- (3) Li, D. Y.; Wu, Y. Y.; Kim, P.; Shi, L.; Yang, P. D.; Majumdar, A. *Appl. Phys. Lett.* **2003**, *83*, 2934–2936.
- (4) Peng, K. Q.; Xu, Y.; Wu, Y.; Yan, Y. J.; Lee, S. T.; Zhu, J. *Small* **2005**, *1*, 1062–1067.
- (5) Maiolo, J. R.; Kayes, B. M.; Filler, M. A.; Putnam, M. C.; Kelzenberg, M. D.; Atwater, H. A.; Lewis, N. S. *J. Am. Chem. Soc.* **2007**, *129*, 12346.
- (6) Dalchiele, E. A.; Martin, F.; Leinen, D.; Marotti, R. E.; Ramos-Barrado, J. R. *J. Electrochem. Soc.* **2009**, *156*, K77–K81.
- (7) Goodey, A. P.; Eichfeld, S. M.; Lew, K. K.; Redwing, J. M.; Mallouk, T. E. *J. Am. Chem. Soc.* **2007**, *129*, 12344.
- (8) Peng, K. Q.; Wang, X.; Lee, S. T. *Appl. Phys. Lett.* **2008**, *92*, 163103.
- (9) Fang, H.; Li, X. D.; Song, S.; Xu, Y.; Zhu, J. *Nanotechnology* **2008**, *19*, 255703.
- (10) Sivakov, V.; Andra, G.; Gawlik, A.; Berger, A.; Plentz, J.; Falk, F.; Christiansen, S. H. *Nano Lett.* **2009**, *9*, 1549–1554.
- (11) Tsakalakos, L.; Balch, J.; Fronheiser, J.; Korevaar, B. A.; Sulima, O.; Rand, J. *Appl. Phys. Lett.* **2007**, *91*, 233117.
- (12) Kalita, G.; Adhikari, S.; Aryal, H. R.; Afre, R.; Soga, T.; Sharon, M.; Koichi, W.; Umeno, M. *J. Phys. D* **2009**, *42*, 115104.
- (13) Barnes, T. M.; Wu, X.; Zhou, J.; Duda, A.; van de Lagemaat, J.; Coutts, T. J.; Weeks, C. L.; Britz, D. A.; Glatkowski, P. *Appl. Phys. Lett.* **2007**, *90*, 243503.
- (14) Contreras, M. A.; Barnes, T.; van de Lagemaat, J.; Rumbles, G.; Coutts, T. J.; Weeks, C.; Glatkowski, P.; Levitsky, I.; Peltola, J.; Britz, D. A. *J. Phys. Chem. C* **2007**, *111*, 14045–14048.
- (15) Miller, A. J.; Hatton, R. A.; Chen, G. Y.; Silva, S. *Appl. Phys. Lett.* **2007**, *90*, 023105.
- (16) Somani, P. R.; Somani, S. P.; Umeno, M. *Appl. Phys. Lett.* **2008**, *93*, 033315.
- (17) Sgobba, V.; Guldi, D. M. *J. Mater. Chem.* **2008**, *18*, 153–157.
- (18) Berson, S.; de Bettignies, R.; Bailly, S.; Guillerez, S.; Jousselme, B. *Adv. Funct. Mater.* **2007**, *17*, 3363–3370.
- (19) Kongkanand, A.; Dominguez, R. M.; Kamat, P. V. *Nano Lett.* **2007**, *7*, 676–680.
- (20) Hu, J. T.; Ouyang, M.; Yang, P. D.; Lieber, C. M. *Nature* **1999**, *399*, 48–51.
- (21) Wei, J. Q.; Jia, Y.; Shu, Q. K.; Gu, Z. Y.; Wang, K. L.; Zhuang, D. M.; Zhang, G.; Wang, Z. C.; Luo, J. B.; Cao, A. Y.; Wu, D. H. *Nano Lett.* **2007**, *7*, 2317–2321.
- (22) Jia, Y.; Wei, J. Q.; Wang, K. L.; Cao, A. Y.; Shu, Q. K.; Gui, X. C.; Zhu, Y. Q.; Zhuang, D. M.; Zhang, G.; Ma, B. B.; Wang, L. D.; Liu, W. J.; Wang, Z. C.; Luo, J. B.; Wu, D. *Adv. Mater.* **2008**, *20*, 4594–4598.
- (23) Peng, K. Q.; Yan, Y. J.; Gao, S. P.; Zhu, J. *Adv. Mater.* **2002**, *14*, 1164–1167.
- (24) Jia, Y.; Wei, J. Q.; Shu, Q. K.; Chang, J. G.; Wang, K. L.; Wang, Z. C.; Luo, J. B.; Liu, W. J.; Zheng, M. X.; Wu, D. H. *Chin. Sci. Bull.* **2007**, *52*, 997–1000.
- (25) Tsakalakos, L.; Balch, J.; Fronheiser, J.; Shih, M. Y.; LeBoeuf, S. F.; Pietrzykowski, M.; Codella, P. J.; Korevaar, B. A.; Sulima, O.; Rand, J.; Davuluru, A.; Rapol, U. *J. Nanophoton.* **2007**, *1*, 013552.
- (26) Gabor, N. M.; Zhong, Z. H.; Bosnick, K.; Park, J.; McEuen, P. L. *Science* **2009**, *325*, 1367–1371.
- (27) Saito, R.; Fujita, M.; Dresselhaus, G.; Dresselhaus, M. S. *Mater. Sci. Eng., B* **1993**, *B19*, 185–191.
- (28) Zhang, M.; Fang, S. L.; Zakhidov, A. A.; Lee, S. B.; E, A. A.; Williams, C. D.; Atkinson, K. R.; Baughman, R. H. *Science* **2005**, *309*, 1215–1219.
- (29) Lombardi, I.; Hochbaum, A. I.; Yang, P. D.; Carraro, C.; Maboudian, R. *Chem. Mater.* **2006**, *18*, 988–991.
- (30) Shimizu, T.; Xie, T.; Nishikawa, J.; Shingubara, S.; Senz, S.; Gösele, U. *Adv. Mater.* **2007**, *19*, 917–920.

NL902581K